

Benchmarking person re-identification datasets and approaches for practical real-world implementations

Jose Huaman, Felix O. Sumari, Luigy Machaca, Esteban Clua and Joris Guerin

¹ Instituto de Computação, Universidade Federal Fluminense, Niteroi-RJ, Brazil

² LAAS-CNRS, Université de Toulouse, Toulouse, France

{jmhacruz, fsumari, luigyarcana}@id.uff.br, esteban@ic.uff.br, jorisguerin.research@gmail.com

Keywords: Person Re-Identification, Practical Deployment, Benchmark Study

Abstract: Recently, Person Re-Identification (Re-ID) has received a lot of attention. Large datasets containing labeled images of various individuals have been released, allowing researchers to develop and test many successful approaches. However, when such Re-ID models are deployed in new cities or environments, the task of searching for people within a network of security cameras is likely to face an important domain shift, thus resulting in decreased performance. Indeed, while most public datasets were collected in a limited geographic area, images from a new city present different features (e.g., people’s ethnicity and clothing style, weather, architecture, etc.). In addition, the whole frames of the video streams must be converted into cropped images of people using pedestrian detection models, which behave differently from the human annotators who created the dataset used for training. To better understand the extent of this issue, this paper introduces a complete methodology to evaluate Re-ID approaches and training datasets with respect to their suitability for unsupervised deployment for live operations. This method is used to benchmark four Re-ID approaches on three datasets, providing insight and guidelines that can help to design better Re-ID pipelines in the future.

This paper is the extended version of our short paper accepted in VISAPP - 2023.

1 INTRODUCTION

As many cameras are being deployed in public places (airports, malls, etc.), monitoring of video streams by security agents becomes impractical. Automated processing is a promising perspective to analyze the whole network in real-time, and select only relevant sequences for verification by human operators. This paper deals with person Re-Identification (Re-ID), a computer vision problem to find an individual in a network of non-overlapping cameras (Bedagkar-Gala and Shah, 2014). It has diverse potential applications such as suspect searching (Liao et al., 2014), identifying owners of abandoned luggage (Altunay et al., 2018), or recovering missing children (Deb et al., 2021). In the literature, the problem of Re-ID is studied under different settings (see Section 2.1). On the one hand, the most studied Re-ID paradigm, which we refer to as *standard Re-ID*, tries to find images representing the query person within a gallery of pre-cropped images of persons, containing at least one

correct match (Lavi et al., 2020). On the other hand, we recently introduced a setting considering specifically the constraints to implement Re-ID for live operations, which we call as *live Re-ID* (Sumari et al., 2020). The first contribution of this paper is to formalize the definition and constraints associated with live Re-ID and to extend the evaluation metrics presented in (Sumari et al., 2020) to facilitate interpretation.

Standard Re-ID is not the best-suited paradigm for practical implementations, as it does not consider the influence of domain shift due to pedestrian detection errors or deployment in a city with different characteristics. Indeed, in our previous experiments (Sumari et al., 2020), we showed that training a successful Re-ID model with respect to standard Re-ID metrics does not guarantee good performance when evaluated in a specific live Re-ID context. Nevertheless, most publicly available large-scale datasets for Re-ID focus on the standard Re-ID setting, and many successful approaches have been developed for this specific purpose. For this reason, we believe that it is essential to study if these datasets and approaches can be used to implement and deploy practical applications in different contexts. More specifically, the objective of this paper is to answer the following questions:

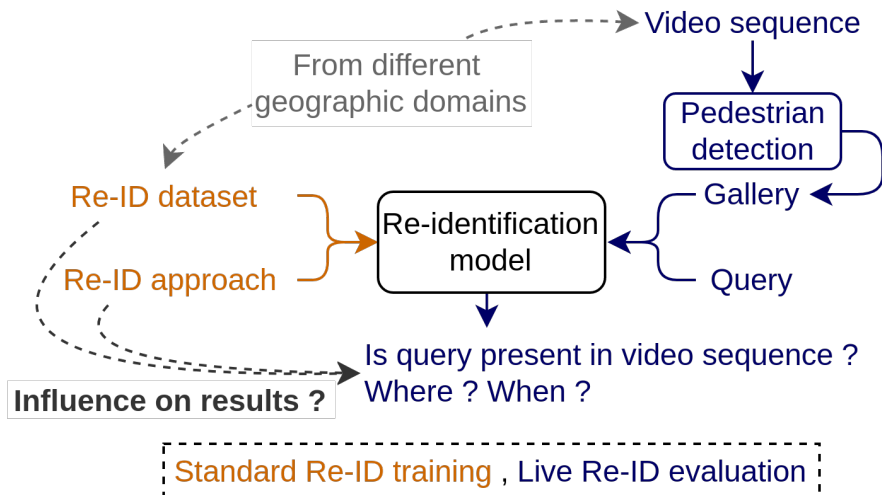


Figure 1: **Conceptual overview.** Representation of the objectives of our benchmark study. This work aims at evaluating how different standard Re-ID approaches and training datasets behave for practical deployment in new environments (live Re-ID).

1. Which characteristics of a standard Re-ID dataset (diversity, size) are most important to train standard Re-ID models for the live Re-ID setting?
2. Which standard Re-ID approaches can be successfully deployed for practical implementations in the live Re-ID setting?
3. Do different Re-ID approaches have different optimal datasets for deployment?
4. Can we use a simple cross-dataset evaluation methodology to assess the deployability of a given approach-dataset pair?

To answer these questions, we conducted a study using three standard Re-ID training datasets and four recent standard Re-ID approaches. For each approach-dataset pair, the Re-ID model obtained was evaluated against the other two datasets and against another one configured for the live Re-ID setting. We also combine training datasets to investigate how dataset size and diversity influence the generalization of the obtained standard Re-ID model. A conceptual overview of our objectives is represented in Figure 1.

In this paper, we consider the evaluation of Re-ID models without additional training on images from the target domain. More sophisticated approaches have been proposed for domain adaptation of standard Re-ID models. On the one hand, the unsupervised domain adaptation problem consists in leveraging unlabeled data from the target domain to improve the performance of the standard Re-ID model (Zhao et al., 2020; Mekhazni et al., 2020). On the other, methods from the transfer learning field (Zhao et al., 2020) have been applied to fine-tune standard Re-ID models for new contexts where a small amount of labeled data

is available (Chen et al., 2018). Such domain adaptation approaches are not tested in this work, but we believe standard Re-ID models performing well without target domain training (our experiments) are likely to be good initialization for more sophisticated fine-tuning approaches. On another note, it was shown that considering bounding box extraction and Re-ID separately is not as good as end-to-end approaches for person search, i.e., galleries of whole scene images (Xiao et al., 2017). However, our results show that this two-step approach can perform well on the live Re-ID setting for some configurations. Likewise, we believe that the results from our study can be useful to pre-train successful initial live Re-ID models and to guide the development of more complex end-to-end architectures for live Re-ID.

This paper is organized as follows: Section 2 discusses the relevant related literature. The proposed benchmark methodology is detailed in Section 3. The results are presented in Section 4 and discussed in Section 5. Finally, Section 6 presents our conclusions.

2 RELATED WORK

A complete literature review of Re-ID approaches is not the purpose of this paper. Instead, we present clear definitions of the different existing Re-ID settings and discuss existing benchmark studies about Re-ID.

2.1 Person re-identification settings

The field of Re-ID consists in retrieving instances of a given individual, called the *query*, within a complex

set of multimedia content called the *gallery* (Gheisari et al., 2006). Different settings are defined by how they represent the query and the gallery items, the constraints on the gallery content, the boundaries of the Re-ID system, and the evaluation methodology.

2.1.1 Popular settings

Standard Re-ID In this setting, both the query, and all items in the gallery are well-cropped images representing entire human bodies. It is sometimes called closed-set Re-ID as it assumes that the query has at least one representative in the gallery. According to the statistics in Papers with Code (Papers with Code, 2021) it is the most studied Re-ID setting by a large margin, in terms of number of papers, datasets and benchmarks published. Some standard Re-ID datasets and successful methods are used for our benchmark study and presented in Section 3. For a more complete overview of standard Re-ID approaches, see (Ye et al., 2021).

Person search This setting consists in replacing the gallery items by whole scene images (Xiao et al., 2017). In other words, a person search model must return the index of the gallery image where the query is present and its location in terms of Bounding Box (BB) coordinates. A survey about person search approaches was proposed in (Islam, 2020).

Open-set Re-ID This setting differs from standard Re-ID in that there is no guarantee that the query is represented in the gallery, i.e., an open-set Re-ID model should be able to answer whether the gallery contains the query. The reader can refer to (Leng et al., 2019) for an overview of recent approaches.

Video-based Re-ID In this setting, images (query and gallery) are replaced by image sequences extracted from consecutive video frames. Sequences are composed of well-cropped entire body images representing the same person. A complete survey of video-based Re-ID was proposed in (Ye et al., 2021).

Others For completeness, we mention other Re-ID variants, namely unsupervised Re-ID (Yang et al., 2021), semi-supervised Re-ID (Moskvayak et al., 2021), human-in-the-loop Re-ID (Wang et al., 2016), or federated Re-ID (Zhuang et al., 2020). However, their specificity lie in Re-ID models training while the other settings above focus on constraints at inference.

2.1.2 Live Re-ID setting

In this section, we clearly define and formalize the *live Re-ID* setting, which is inspired by our previous work (Sumari et al., 2020). It takes into account all relevant aspects for deploying Re-ID in practical real-world applications. An overview of the live Re-ID workflow can be seen in Figure 2.

When looking for a query person during live operations, whole scene videos need to be processed in near real-time, hence the galleries for live Re-ID are composed of the consecutive *whole scene frames* from *short video sequences*. The live Re-ID context is also highly *open-set* as the probability to have the query in a short video sequence from a given camera is low. Hence, this setting combines elements from several of the Re-ID settings mentioned above. Using these live Re-ID characteristics, it was recently shown that using tracking and anomaly detection to reduce the size of the generated gallery improves live Re-ID results (Machaca et al., 2022).

Another key characteristic of live Re-ID is that the training context is different from the deployment context. Indeed, building new specialized datasets for deployment in every shopping mall or small city is unrealistic from the perspective of future advances in the field. This highlights the importance of studying *cross domain* transfer of Re-ID, which was first discussed and highlighted in (Luo et al., 2020).

Finally, this setting also takes into account that Re-ID model predictions need to be *processed by a human agent*, who triggers appropriate actions. This way, very high rank-1 accuracy is not mandatory for live Re-ID, as the operator can find the query in later ranks. On the other hand, false alarm rates must be kept low to avoid overloading human operators. To evaluate these two objectives, we introduced two evaluation metrics representing both dimensions of the problem in (Sumari et al., 2020). The experiments conducted in this paper aim at studying the transferability of standard Re-ID approaches and datasets for deployment in the live Re-ID setting.

2.2 Person re-identification benchmarks

This section presents several benchmark studies considering different aspects of the Re-ID pipeline.

A large scale benchmark experiment was conducted to compare various approaches for standard and video-based Re-ID (Gou et al., 2018). They evaluated more than 30 approaches on 16 public datasets, and produced the largest Re-ID benchmark to date. In addition, they built a new dataset to represent several constraints for real-world implementations, such

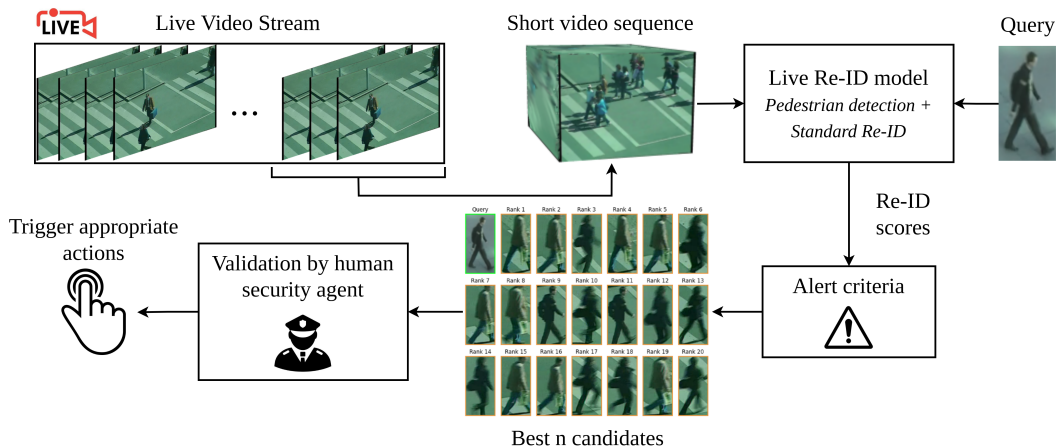


Figure 2: **The live Re-ID setting.** When deploying Re-ID models in practice, the galleries are composed of whole scene video sequences. When an alert is raised, the data are verified by a security agent to decide whether actions should be triggered.

as pedestrian detection errors and illumination variations, among others. However, they do not consider cross domain performance and all evaluations are conducted in the closed-set setting, which are major limitations regarding future deployments. In addition, a smaller systematic evaluation of video-based Re-ID approaches was proposed in (Zheng et al., 2016).

Another extensive set of experiments was conducted to evaluate different pedestrian detection models on a two-step person search pipeline (Zheng et al., 2017). They demonstrated that the best models on standard object detection metrics are not necessarily the best suited for Re-ID from whole scene frames. In addition, a first benchmark regarding cross-domain transfer of Re-ID approaches was proposed in (He et al., 2020). Their experiments consisted in training an approach on one standard Re-ID dataset and evaluating on another. Finally, on another note, different approaches for federated Re-ID where compared in (Zhuang et al., 2020).

The studies presented above have brought valuable insights to the Re-ID community. However, none of them allows to assess the performance of a Re-ID model against all the challenges involved during deployment in a new environment for practical use in security applications. Our paper contributes to bridging this gap by conducting experiments within the live Re-ID setting, which was designed to take into account all these challenges. In particular, we consider the influence of different standard Re-ID approaches and training datasets on live Re-ID results.

3 BENCHMARK METHODOLOGY

The objective of this paper is to study if different standard Re-ID approaches and training datasets can be used to build efficient live Re-ID pipelines, ready for practical deployment. This section presents the different components of the proposed benchmarking evaluation, i.e., the compared datasets and approaches, metrics used, and experiments conducted.

3.1 Datasets

In our experiments, we used three public datasets to train and evaluate standard Re-ID models, and a live Re-ID dataset to evaluate the trained Re-ID models within the context of live operations. Figure 3 shows example images from the datasets, where we can see that they represent people from different geographic regions, under different resolutions, lighting conditions, and camera angles.

3.1.1 Standard Re-ID datasets

This section presents briefly the standard Re-ID datasets used in this study. Table 1 summarizes relevant statistics.

Market-1501 This dataset was collected at a supermarket in Tsinghua University, Beijing, China (Zheng et al., 2015a). The cropped images are detected automatically using a Deformable Part Model (Felzenszwalb et al., 2009), which outputs are filtered manually to keep only good BB representing human bodies. This automated way of extracting BB is closer to realistic settings, which might improve live Re-ID results

Table 1: **Standard Re-ID training datasets.** Characteristics of the standard Re-ID datasets used in this paper.

Dataset	# Cameras	Split	Input type	# IDs	# Images
CUHK03	2	Train	–	767	7368
		Test	Query	700	1400
			Gallery	700	5328
DukeMTMC	8	Train	–	702	16522
		Test	Query	702	2228
			Gallery	1110	17661
Market-1501	6	Train	–	751	12936
		Test	Query	750	3368
			Gallery	751	15913



(e) m-PRID. Extracted from PRID-2011 videos using YOLO-V3. Blue indicates good images for standard Re-ID, while red BB are likely to generate Re-ID errors.

Figure 3: **Benchmarking datasets.** Example images from the datasets used in our experimental study.

for models trained on Market-1501. As illustrated by Figure 3a, cropped images appear to present a high level of details about the people represented (i.e., images are taken from a close perspective or videos are high resolutions). Lighting conditions in this dataset are also good to distinguish specific features.

DukeMTMC This dataset was collected at the Duke University campus, Durham, North Carolina, USA (Ristani et al., 2016). The BB in DukeMTMC are hand drawn, lighting conditions are good but resolution of the BB is relatively low (Figure 3b).

CUHK03 This dataset was built using video footage collected at the campus of the Chinese University of Hong Kong (Li et al., 2014). In our work, we used the manually labeled version of the BB. Cropped images are high resolution but illumination is dark, which reduces images quality (Figure 3c).

3.1.2 Live Re-ID dataset

To evaluate the different standard Re-ID models for the live Re-ID setting, we used the same dataset as our previous work (Sumari et al., 2020), which we call *m-PRID*. It is a modified version of PRID-2011 (Hirzer et al., 2011), built from the raw video footage and the original annotations that were used to create the official curated version of PRID-2011¹. The videos were collected from two non-overlapping cameras (A and B), located in Graz, Austria. This way, compared to the training datasets above, evaluation on m-PRID represents a geographic domain shift. In total PRID-2011 contains 385 different identities for camera A and 749 for camera B, of which 200 identities appear in both cameras. The m-PRID dataset is composed of several two minutes videos (30 from A and 33 from B). For each short video sample, a ground truth file gather information about each person it contains (identifier, frames where it appears, bounding box coordinates). For evaluation, a total of 73 queries are considered.

To better grasp the influence of the pedestrian detection model, we also evaluate our different models on the original PRID-2011 dataset for standard Re-ID. Figure 3d shows cropped images of poor resolution.

¹We thank the authors of PRID-2011 for their help.

tion, taken from relatively high camera angle compared to other datasets. This way, we can see if performance decrease on the live Re-ID setting are due to the domain shift of PRID or to the pedestrian detector inaccuracies (Figure 3e).

3.2 Re-ID approaches evaluated

This work studies the performance of four successful standard Re-ID approaches. To complement previous benchmark studies (Section 2.2), only recent approaches are selected for this work.

3.2.1 Bag of Tricks (BoT)

The *Bag of Tricks* approach resulted from the observation that most improvements for Re-ID baselines come from neural network training tricks rather than Re-ID approaches themselves (Luo et al., 2019). As a result, they came up with a simple recipe to successfully train standard Re-ID models on top of a ResNet-50 backbone (He et al., 2015). In particular:

1. the model is pretrained on ImageNet,
2. the dimension of the fully connected layer is set to the number of training identities,
3. the batch size is set to 64,
4. images are resized to 256 X 128,
5. both triplet and cross entropy loss are used, and
6. Adam is adopted for optimization.

3.2.2 Strong Baseline and Batch Normalization Neck (SBS)

This approach (Luo et al., 2020) extended BoT by adding the following tricks:

1. a warm-up strategy (Fan et al., 2019) is applied to bootstrap the network,
2. random erasing augmentation (Zhong et al., 2017) is used to account for potential occlusion,
3. label smoothing (Szegedy et al., 2015) is used to reduce overfitting,
4. the last stride of the ResNet-50 backbone is set to 1 to increase spatial resolution,
5. batch normalization layers are added, and
6. a new center loss is introduced to account for the clustering effect of tracking.

3.2.3 Attention Generalized mean pooling with Weighted triplet loss (AGW)

This technique (Ye et al., 2021) was also designed on top of BoT with three major improved components:

1. a powerful non-local attention block is developed to mix the part and global attention features,
2. a learnable pooling layer replaces max and average pooling to better capture the domain-specific discriminative features,
3. the use of weighted regularization triplet loss inherits the advantages of relative distance optimization between positive and negative pairs without introducing additional parameters.

3.2.4 Multiple Granularity Network (MGN)

This approach (Wang et al., 2018) was designed combines local and global information in different image granularity. Its specificities are:

1. a strategy to learn local feature representations by splitting the input image in horizontal stripes. Then, the ResNet-50 backbone is divided into a multiple branches after the fourth residual stage.
2. a strategy to learn global features using a global branch using down-sampling with a stride-2 convolution layer and representations with 256 dimension features. The part-N branch has a similar architecture without down-sampling.
3. a new Loss functions, combining Softmax for classification and triplet loss for metric learning.

3.3 Proposed experiments

To compare the Re-ID datasets and approaches presented above, several experiments are conducted.

3.3.1 Single dataset evaluation

We first evaluate each approach and dataset pair individually. The standard Re-ID approach is simply fitted to the training split of the dataset, and evaluated on the testing split. The quality of the Re-ID model’s predictions on the testing set is assessed using standard Re-ID metrics, coming from the field of information retrieval:

Rank-n This metric represents the proportion of queries for which at least one correct match was predicted within the n highest ranked gallery images (Moon and Phillips, 2001). In practice, we report results for $n \in \{1, 5, 10\}$. This metric represents the Re-ID model’s ability to retrieve the easiest match.

mAP The *mean average precision* for Re-ID takes into account the predicted ranks of all existing matches (Zheng et al., 2015b). To have a perfect mAP, all the gallery images corresponding to the query need

to be ranked in the first places. It is the average performance across all instances of the query.

mINP The *mean inverse negative penalty* reflects the position of the worst ranked match from the gallery (Ye et al., 2021). It represents the capacity of a Re-ID model to find all instances of the query in the gallery.

These three metrics represent different skills of a Re-ID model. Computing them might help understand which of these skill is important regarding generalization to new contexts and to more complex real-world scenarios, i.e., live Re-ID in different cities.

3.3.2 Cross-dataset evaluation

A simple cross-dataset experiment is also conducted (He et al., 2020). It consists in training an approach on one of the three standard Re-ID datasets, and evaluating it on the other two. The same metrics are used (rank-n, mAP and mINP). As the datasets were built in different geographic areas, these results can give first insights about domain generalization of the different training datasets and approaches. Conducting such cross-dataset evaluation is also much easier than evaluating the system in the live Re-ID setting. Hence, another objective of this experiment is to discover if simple cross-dataset evaluation can be used as a proxy to quickly test new datasets and approaches for live implementations. In other words, we want to know if there is correlation between cross-dataset results and live Re-ID results of dataset-approach pairs.

For the cross-datasets experiments, we also try to combine training datasets to see if it improves test performance. In the COMBINED_{all} experiments, training is conducted on all training sets available (Market-1501, DukeMTMC and CUHK03), including the one corresponding to the test set of interest. This allows to evaluate if adding data from other sources can help improving standard Re-ID in the traditional supervised setting. In the COMBINED_{others} experiments, the training set corresponding to the test dataset is excluded. For example, when evaluating on CUHK03, the standard Re-ID models are trained on Market-1501 and DukeMTMC. Finally, the COMBINED_{scaled} setting is similar to COMBINED_{others}, but we ensure that the total number of training data is equal to the number of data in the largest dataset.

For example, when combining datasets A and B , respectively of size N_A and N_B , we only take fractions N_A^* and N_B^* of each datasets such that $N_A^* + N_B^* = \max(N_A, N_B)$ and $N_A^* = N_B^*$. Comparing COMBINED_{scaled}, with COMBINED_{others} allows

to evaluate how size and diversity affect the generalization power of a dataset. For evaluations on PRID-2011, which is not among the training datasets, COMBINED_{all} and COMBINED_{others} are identical and referred to as COMBINED. When evaluating on CUHK03, the COMBINED_{scaled} dataset is composed of 8261 images from DukeMTMC and 8261 from Market-1501. When evaluating on DukeMTMC it contains 6468 images from both CUHK03 and Market-1501, and when evaluating on Market-1501 it contains 9754 images from DukeMTMC and 7368 images from CUHK03. Finally, when evaluating on PRID-2011, COMBINED_{scaled} is composed of 5507 images from CUHK03, 5508 from DukeMTMC and 5507 from Market-1501.

3.3.3 Live Re-ID evaluation

Finally, each standard Re-ID approach and dataset pairs are evaluated in the live Re-ID setting using the m-PRID dataset. We apply the evaluation methodology from (Sumari et al., 2020). For each short video sequence, Bounding Boxes (BB) of pedestrians are extracted using a YOLO-V3 object detector (Redmon and Farhadi, 2018), trained on COCO (Lin et al., 2015) and available in TensorFlow (Abadi et al., 2015). The score threshold used to decide which predicted BB to keep is set to 0.5. Then, the trained standard Re-ID approaches are applied to the gallery composed of these BB. Following the notations of (Sumari et al., 2020), the length of video sequences evaluated τ is set to 1000 frames and the number of candidates shown to the monitoring agent η is set to 20. These values generated best results by a large margin in their experiments. For the threshold β on Re-ID scores used to generate alerts, we test all values between 0 and 1 with a step size of 0.02.

To compare the different models, we use the live Re-ID metrics introduced in (Sumari et al., 2020). On the one hand, the *Finding Rate* (FR) represents the proportion of videos where the query was present, such that an alert was shown to the agent and where the query was among the selected candidates. A low FR means that the query was missed frequently. On the other, the *True Validation Rate* (TVR) represents the proportion of alert shown to the monitoring agent in which the query was present among the candidates. A low TVR means that the agent was frequently disturbed for no reason, which can be problematic when many cameras need to be monitored simultaneously.

In this paper we also propose two new metrics to represent the performance of a live Re-ID approach with a single number, to facilitate comparisons and interpretation. The first one is based on the observation that the meanings of FR and TVR are respectively

very close to recall and precision. This way, similarly to object detection evaluation, we can plot *TVR vs FR* curves and compute the *mean Average Precision* (mAP) as the area under the curve. The second unified metric consists in computing a weighted harmonic mean of FR and TVR, similarly to the F-score computation for precision and recall. We call the resulting metric F_γ , which is defined as follows:

$$F_\gamma = (1 + \gamma^2) \cdot \frac{\text{FR} \cdot \text{TVR}}{(\gamma^2 \cdot \text{FR}) + \text{TVR}}. \quad (1)$$

In practice, we compute F_γ for $\gamma \in \{0.5, 1, 2\}$. In $F_{0.5}$, we consider that having a high TVR is two times more important than a high FR. In F_2 , we consider FR two times more important than TVR, and in F_1 FR and TVR contribute equally to the results. However, for each value of the threshold β , there is a different corresponding value of F_γ . To solve this issue, we use the same approach as Guérin et al., (Guérin et al., 2020) consisting in evaluating a model by its performance at the optimal configuration. The result is called *optimal* F_γ (F_γ^*), and corresponds to the highest F_γ across values of β . The value of β corresponding to F_γ^* can be viewed as the operating point of the Re-ID model, which can be obtained by quick experiments in the practical implementation context. An F_γ^* score of 1 means that there exist a Re-ID threshold β such that it always finds the query when it is in the video sequence, but never raises alerts when it is not.

The objective of these experiments is to see if the best approaches and datasets from previous experiments are also the best ones from the perspective of practical implementation in new cities.

Combined datasets experiments are also conducted for the live Re-ID setting. However, as PRID-2011 is not one of the training datasets used in our experiments, $\text{COMBINED}_{\text{all}}$ and $\text{COMBINED}_{\text{others}}$ are actually equivalent here and simply referred to as COMBINED . They are also compared against $\text{COMBINED}_{\text{scaled}}$ results to study the impact of dataset size and diversity. The $\text{COMBINED}_{\text{scaled}}$ training dataset for live Re-ID experiments on m-PRID are composed of 5507 images from CUHK03, 5508 from DukeMTMC and 5507 from Market-1501.

4 RESULTS

In order to improve clarity, only a condensed version of the results is presented. The complete results can be found at: https://github.com/josemiki/benchmarking_person_Re_ID. It contains all the results from cross-dataset evaluation, contains the missing metrics and the TVR vs FR curves for live Re-ID

evaluations. Overall, the curated results presented in the core paper are representative of the complete results and are sufficient to draw our conclusions.

The results for single dataset evaluation are reported in Table 2. The results obtained are good: rank-1 and mAP are around 70% for the worst approach on the most difficult dataset. They are also relatively homogeneous: for each dataset-metric pairs, all four methods perform similarly (less than 10% difference). The results obtained show that the tested approaches generalize differently to new contexts. For instance training MGN on Market-1501 leads to 47% rank-10 accuracy on CUHK03, while the same experiment using BoT only reaches 15%. For comparison, when training was conducted on CUHK03 itself, only a 3% difference was observed between the approaches (Table 2). The choice of the training dataset is also important, e.g., when training MGN for CUHK03, Market-1501 is 13% better than DukeMTMC.

The cross-dataset evaluation results are presented in Table 3. We only report Rank-10 for two reasons. First, the complete results show that the ranking of approaches is stable under different values of n . Second, having a high Rank-10 is more important than lower ranks for live Re-ID, as explained in Section 2.1.2.

Finally, the live Re-ID evaluation results are presented in Table 4. They also illustrate that it is crucial to properly select the training dataset and approach for such task transfer. Overall, MGN appears to generalize much better for use in a live Re-ID setting. For training, Market-1501 appears to work best for most approaches except MGN. The best combination using a single dataset is MGN trained on DukeMTMC, reaching a mAP of 0.72 and an optimal F1 of 0.76.

5 DISCUSSION

In this section, we propose to discuss the results obtained in our study, highlighting several key insights regarding training standard Re-ID models for cross-domain live Re-ID.

5.1 Impact of the training dataset

Proper selection of the training dataset clearly influences the results in a different evaluation domain. However, there is no clear winner between Market-1501 and DukeMTMC to know which individual dataset should be used for any context. In addition, the cross-dataset results do not allow to choose the best individual dataset for training models for the live Re-ID setting. Indeed, Table 3 suggested that the best dataset for MGN should be Market-1501, whereas it

Table 2: **Single dataset evaluations.** Results obtained by training and evaluating Re-ID approaches with the train and test splits of the same dataset. For each dataset, the best Re-ID approach is in bold.

Dataset	Approach	Rank-1	Rank-5	Rank-10	mAP	mINP
CUHK03	AGW	0.73	0.88	0.92	0.72	0.63
	MGN	0.78	0.91	0.95	0.76	0.66
	SBS	0.74	0.89	0.93	0.73	0.62
	BoT	0.69	0.86	0.92	0.67	0.55
DukeMTMC	AGW	0.89	0.95	0.97	0.80	0.46
	MGN	0.91	0.96	0.97	0.82	0.47
	SBS	0.89	0.95	0.96	0.79	0.44
	BoT	0.87	0.94	0.96	0.77	0.41
Market-1501	AGW	0.95	0.99	0.99	0.88	0.66
	MGN	0.96	0.99	0.99	0.89	0.66
	SBS	0.95	0.98	0.99	0.88	0.66
	BoT	0.94	0.98	0.99	0.86	0.61

is outperformed by DukeMTMC for live Re-ID (Table 4). In the remaining of this section, we discuss the results obtained on the combined datasets settings to gain new insights regarding building standard Re-ID datasets for efficient training of live Re-ID models.

5.1.1 Can data from a different domain improve results in the standard Re-ID scenario ?

To answer this question, we compare results from Table 2 and the COMBINED_{all} rows in Table 3. Overall, for both Rank-10 and mAP, the results for COMBINED_{all} appear slightly better than the results obtained when learning only on the training set of the evaluated dataset. To illustrate this, we computed the mean and standard deviation across all evaluation dataset and approaches. When using only the training set we obtain the following results: $R10 = 0.962 \pm 0.026$ and $mAP = 0.798 \pm 0.068$. When combining the three available datasets for training we have: $R10 = 0.964 \pm 0.022$ and $mAP = 0.805 \pm 0.067$.

To confirm this intuition, we conduct a Paired Sample T-Test to determine whether the mean difference between the results obtained using the single in-domain training set and the COMBINED_{all} are statistically significant. The p-values obtained are 0.2750 for R10 and 0.2313 for mAP, suggesting that the Null Hypothesis cannot be rejected, i.e., *we cannot conclude that using more data from a different domain is beneficial to the standard Re-ID training process.*

5.1.2 Between dataset size and diversity, which is most important for cross-domain generalization ?

The first question we want to answer is whether combining datasets from different domains can help cross domain generalization. To evaluate this, we can compare the results for COMBINED_{others} (COMBINED

for PRID-2011) against the results from the best individual dataset in Table 3. The mean and standard deviation across all evaluation dataset and approaches are $R10 = 0.509 \pm 0.242$ and $mAP = 0.224 \pm 0.099$ for the best individual dataset, and $R10 = 0.580 \pm 0.241$ and $mAP = 0.297 \pm 0.124$ when combining all the available training datasets (except the one corresponding to the evaluated test set). The Paired Sample T-Test gives p-values of 0.0001 for both R10 and mAP, which is extremely statistically significant. In other words, our experiments confirm that *combining several training datasets from different domains allows to train Re-ID models that generalize better to new unknown domains.*

We then want to know if simply increasing the diversity in the training dataset without increasing its size also help for cross domain generalization. To evaluate this, we can compare the results for COMBINED_{scaled} against the results from the best individual dataset in Table 3. As a reminder, COMBINED_{scaled} consists in building a training dataset by taking data from all available training sets (except the one corresponding to the evaluated test set) in such a way that the total number of training data does not exceed that size of the largest individual training set. The mean and standard deviation across all evaluation dataset and approaches are $R10 = 0.509 \pm 0.242$ and $mAP = 0.224 \pm 0.099$ for the best individual dataset, and $R10 = 0.555 \pm 0.245$ and $mAP = 0.279 \pm 0.125$ for COMBINED_{scaled}. The Paired Sample T-Test gives p-values of 0.0001 for R10 and 0.0005 for mAP, which is extremely statistically significant. In other words, our experiments confirm that *increasing diversity in training dataset, even without increasing its size, allows to train Re-ID models that generalize better to new domains.*

In view of the two encouraging results presented above, we now want to know whether the size of

Table 3: **Cross-dataset evaluations.** Results obtained by training Re-ID approaches on one dataset and evaluating on another. For each evaluation dataset: the best Re-ID approach for a given dataset is in bold; the best training dataset for a given approach is in blue. R10 means Rank-10.

Evaluation dataset	Training dataset	AGW		MGN		SBS		BoT	
		R10	mAP	R10	mAP	R10	mAP	R10	mAP
CUHK03	Market-1501	0.21	0.08	0.47	0.22	0.40	0.18	0.15	0.04
	DukeMTMC	0.18	0.06	0.34	0.14	0.35	0.13	0.15	0.05
	COMBINED _{all}	0.94	0.71	0.96	0.82	0.94	0.76	0.92	0.68
	COMBINED _{others}	0.32	0.14	0.55	0.27	0.52	0.24	0.28	0.11
	COMBINED _{scaled}	0.31	0.13	0.52	0.23	0.46	0.20	0.23	0.09
DukeMTMC	Market-1501	0.58	0.22	0.77	0.39	0.74	0.34	0.49	0.15
	CUHK03	0.50	0.17	0.70	0.31	0.60	0.21	0.36	0.10
	COMBINED _{all}	0.96	0.79	0.97	0.82	0.96	0.78	0.96	0.77
	COMBINED _{others}	0.65	0.29	0.81	0.44	0.79	0.41	0.55	0.21
	COMBINED _{scaled}	0.62	0.26	0.78	0.40	0.75	0.35	0.51	0.18
Market-1501	DukeMTMC	0.75	0.26	0.87	0.37	0.82	0.31	0.71	0.22
	CUHK03	0.73	0.29	0.86	0.39	0.80	0.34	0.66	0.22
	COMBINED _{all}	0.99	0.88	0.99	0.91	0.99	0.88	0.99	0.86
	COMBINED _{others}	0.83	0.38	0.93	0.52	0.91	0.47	0.80	0.34
	COMBINED _{scaled}	0.83	0.38	0.92	0.52	0.89	0.46	0.78	0.32
PRID-2011	CUHK03	0.18	0.11	0.35	0.26	0.29	0.20	0.13	0.09
	DukeMTMC	0.20	0.12	0.42	0.30	0.26	0.17	0.16	0.07
	Market-1501	0.26	0.19	0.40	0.28	0.30	0.20	0.23	0.13
	COMBINED	0.32	0.20	0.45	0.35	0.33	0.23	0.24	0.15
	COMBINED _{scaled}	0.24	0.18	0.46	0.36	0.36	0.26	0.22	0.15

Table 4: **Live Re-ID evaluation.** Results obtained by training Re-ID approaches on one standard Re-ID dataset and evaluating on m-PRID for the live Re-ID setting. For each training dataset, the best approach is in bold and for each approach, the best dataset is in blue.

Approach	CUHK03		DukeMTMC		Market-1501		COMBINED		COMBINED _{scaled}	
	F_1^*	mAP	F_1^*	mAP	F_1^*	mAP	F_1^*	mAP	F_1^*	mAP
AGW	0.39	0.23	0.40	0.25	0.46	0.33	0.56	0.49	0.49	0.39
BoT	0.27	0.10	0.40	0.22	0.47	0.32	0.45	0.30	0.44	0.31
SBS	0.51	0.43	0.58	0.54	0.60	0.50	0.71	0.71	0.68	0.72
MGN	0.66	0.60	0.76	0.72	0.69	0.63	0.81	0.80	0.77	0.75

the training dataset is actually helping cross-domain generalization or if adding diversity is actually sufficient. To evaluate this, we can compare the results for COMBINED_{others} against the results for COMBINED_{scaled} in Table 3. The mean and standard deviation across all evaluation dataset and approaches are $R10 = 0.580 \pm 0.241$ and $mAP = 0.297 \pm 0.124$ for COMBINED_{others}, and $R10 = 0.555 \pm 0.245$ and $mAP = 0.279 \pm 0.125$ for COMBINED_{scaled}. The Paired Sample T-Test gives p-values of 0.0020 for R10 and 0.0075 for mAP, which is very statistically significant. In other words, our experiments confirm that *adding more data from domains that are already present in the training set help generalization to new unknown domains.*

5.1.3 live Re-ID results

The live ReID results on m-PRID (Table 4) confirm the conclusions drawn from the cross-dataset exper-

iments. In particular, the COMBINED_{scaled} results appear better than the results with a single training set, suggesting the importance of training data diversity for practical live Re-ID implementation in a new context. The COMBINED results are themselves better than COMBINED_{scaled}, which suggest that one should use all the available data to train a good standard Re-ID model for live Re-ID implementation. Finally, we emphasize the good results obtained by training MGN on the COMBINED training dataset. These results are very encouraging after the pessimistic results reported by Sumari et al. (Sumari et al., 2020) for live Re-ID.

5.2 Impact of the standard Re-ID approaches

All the approaches tested in this study perform well in the single dataset scenario. However, when it comes

to generalization to live operation contexts, MGN has a clear advantage against the other three techniques. This conclusion could already be intuited from the cross-dataset experiments, which suggests a simple yet powerful approach to test future standard Re-ID approaches before live deployment. MGN is the only approach involving a specific image splitting, forcing the network to focus on different body part. In view of our results, this property appears to be desirable for generalization to the live Re-ID setting.

Besides MGN, the SBS approach also appear to present much better generalization than its competitors (Table 3 and 4). Hence, a promising research direction for live Re-ID research would be to design a new standard Re-ID architecture combining features from MGN and SBS, as described in Section 3.2.

6 CONCLUSION

6.1 Overview

This paper presents a comprehensive evaluation methodology to benchmark different standard Re-ID approaches and training datasets with respect to their ability to be deployed in practical applications from a different context. To do so, we first formalized the new live Re-ID setting, and define new unified evaluation metrics to facilitate interpretation. The performance of different standard Re-ID models is evaluated on this setting. We also conduct simple cross-dataset experiments to see if it can be used to predict which datasets and approaches will generalize better to the live Re-ID setting.

The main conclusions from this study are:

1. Although previous work reported very pessimistic results,(Sumari et al., 2020) our experiments showed that it is possible to design good live Re-ID pipelines by properly choosing the standard Re-ID model and combining publicly available training dataset.
2. Proper choice of the standard re-ID approach and training dataset can influence greatly the results when transferring the model to the cross-domain live Re-ID setting.
3. Increasing training dataset diversity helps generalization to the cross-domain live Re-ID setting.
4. Increasing training dataset size allows to improve cross-domain generalization even further.
5. Simple cross-dataset evaluation can be used to quickly assess the generalization performance of future standard Re-ID techniques for live Re-ID.

Although we only studied the straightforward transfer strategy without fine-tuning, we believe that the results presented here can serve as a good starting point to develop better live Re-ID models in the future.

6.2 Future work

The outputs of this study suggest several interesting research directions. First, it would be very valuable to build new live Re-ID datasets, allowing not only to confirm the results obtained in this study, but also to see if good live Re-ID performance is consistent across different scenarios. Then, this benchmark experiment can be extended to account for different pedestrian detectors, another important component of the live Re-ID pipeline. In particular, it would be interesting to study if specific Re-ID approaches combine better with specific object detectors.

The evaluation methodology proposed in this paper could help to answer this question. Another valuable contribution would be to create a ready-to-use website implementing the proposed benchmarking methodology for researchers to test their new approaches easily. It would also be interesting to see if existing unsupervised cross-dataset adaptation methods could help generalization to the live Re-ID setting. Finally, it would be interesting to study how the good design choices identified in this study can be leveraged to develop successful end-to-end approaches for live Re-ID.

REFERENCES

- Abadi, M., Agarwal, A., Barham, P., Brevdo, E., Chen, Z., Citro, C., Corrado, G. S., Davis, A., Dean, J., Devin, M., Ghemawat, S., Goodfellow, I., Harp, A., Irving, G., Isard, M., Jia, Y., Jozefowicz, R., Kaiser, L., Kudlur, M., Levenberg, J., Mané, D., Monga, R., Moore, S., Murray, D., Olah, C., Schuster, M., Shlens, J., Steiner, B., Sutskever, I., Talwar, K., Tucker, P., Vanhoucke, V., Vasudevan, V., Viégas, F., Vinyals, O., Warden, P., Wattenberg, M., Wicke, M., Yu, Y., and Zheng, X. (2015). TensorFlow: Large-scale machine learning on heterogeneous systems. Software available from tensorflow.org.
- Altunay, D. G., Karademir, N., Topçu, O., and Direkoğlu, C. (2018). Intelligent surveillance system for abandoned luggage. In *26th Signal Processing and Communications Applications Conf. (SIU)*, pages 1–4. IEEE.
- Bedagkar-Gala, A. and Shah, S. K. (2014). A survey of approaches and trends in person re-identification. *Image and vision computing*, 32(4):270–286.
- Chen, H., Wang, Y., Shi, Y., Yan, K., Geng, M., Tian, Y., and Xiang, T. (2018). Deep transfer learning for person re-identification. In *2018 IEEE Fourth Interna-*

- tional Conference on Multimedia Big Data (BigMM)*, pages 1–5. IEEE.
- Deb, D., Aggarwal, D., and Jain, A. K. (2021). Identifying missing children: Face age-progression via deep feature aging. In *25th International Conference on Pattern Recognition (ICPR)*, pages 10540–10547. IEEE.
- Fan, X., Jiang, W., Luo, H., and Fei, M. (2019). Spheredid: Deep hypersphere manifold embedding for person re-identification. *Journal of Visual Communication and Image Representation*, 60:51–58.
- Felzenszwalb, P. F., Girshick, R. B., McAllester, D., and Ramanan, D. (2009). Object detection with discriminatively trained part-based models. *IEEE transactions on pattern analysis and machine intelligence*, 32(9):1627–1645.
- Gheissari, N., Sebastian, T. B., and Hartley, R. (2006). Person reidentification using spatiotemporal appearance. In *2006 IEEE computer society conference on computer vision and pattern recognition (CVPR'06)*, volume 2, pages 1528–1535. IEEE.
- Gou, M., Wu, Z., Rates-Borras, A., Camps, O., Radke, R. J., et al. (2018). A systematic evaluation and benchmark for person re-identification: Features, metrics, and datasets. *IEEE transactions on pattern analysis and machine intelligence*, 41(3):523–536.
- Guérin, J., de Paula Canuto, A. M., and Goncalves, L. M. G. (2020). Robust detection of objects under periodic motion with gaussian process filtering. In *2020 19th IEEE International Conference on Machine Learning and Applications (ICMLA)*, pages 685–692. IEEE.
- He, K., Zhang, X., Ren, S., and Sun, J. (2015). Deep Residual Learning for Image Recognition. *arXiv:1512.03385 [cs]*. arXiv: 1512.03385.
- He, L., Liao, X., Liu, W., Liu, X., Cheng, P., and Mei, T. (2020). Fastreid: A pytorch toolbox for general instance re-identification. *arXiv preprint arXiv:2006.02631*.
- Hirzer, M., Beleznai, C., Roth, P. M., and Bischof, H. (2011). Person re-identification by descriptive and discriminative classification. In *Scandinavian conference on Image analysis*, pages 91–102. Springer.
- Islam, K. (2020). Person search: New paradigm of person re-identification: A survey and outlook of recent works. *Image and Vision Computing*, 101:103970.
- Lavi, B., Ullah, I., Fatan, M., and Rocha, A. (2020). Survey on reliable deep learning-based person re-identification models: Are we there yet? *arXiv preprint arXiv:2005.00355*.
- Leng, Q., Ye, M., and Tian, Q. (2019). A survey of open-world person re-identification. *IEEE Transactions on Circuits and Systems for Video Technology*, 30(4):1092–1108.
- Li, W., Zhao, R., Xiao, T., and Wang, X. (2014). Deepreid: Deep filter pairing neural network for person re-identification. In *Proceedings of the IEEE conference on computer vision and pattern recognition*, pages 152–159.
- Liao, S., Mo, Z., Zhu, J., Hu, Y., and Li, S. Z. (2014). Open-set person re-identification. *arXiv preprint arXiv:1408.0872*.
- Lin, T.-Y., Maire, M., Belongie, S., Bourdev, L., Girshick, R., Hays, J., Perona, P., Ramanan, D., Zitnick, C. L., and Dollár, P. (2015). Microsoft coco: Common objects in context.
- Luo, H., Gu, Y., Liao, X., Lai, S., and Jiang, W. (2019). Bag of Tricks and a Strong Baseline for Deep Person Re-Identification. In *2019 IEEE/CVF Conference on Computer Vision and Pattern Recognition Workshops (CVPRW)*, pages 1487–1495, Long Beach, CA, USA. IEEE.
- Luo, H., Jiang, W., Gu, Y., Liu, F., Liao, X., Lai, S., and Gu, J. (2020). A Strong Baseline and Batch Normalization Neck for Deep Person Re-identification. *IEEE Transactions on Multimedia*, 22(10):2597–2609. arXiv: 1906.08332.
- Machaca, L., Huaman, J., Clua, E., Guerin, J., et al. (2022). TrADe Re-ID—live person re-identification using tracking and anomaly detection. *21st IEEE International Conference on Machine Learning and Applications (to appear)*.
- Mekhzazni, D., Bhuiyan, A., Ekladios, G., and Granger, E. (2020). Unsupervised domain adaptation in the dissimilarity space for person re-identification. In *European Conference on Computer Vision*, pages 159–174. Springer.
- Moon, H. and Phillips, P. J. (2001). Computational and performance aspects of pca-based face-recognition algorithms. *Perception*, 30(3):303–321.
- Moskvyak, O., Maire, F., Dayoub, F., and Baktashmotlagh, M. (2021). Going deeper into semi-supervised person re-identification. *arXiv preprint arXiv:2107.11566*.
- Papers with Code (2021). person Re-ID. paperswithcode.com/task/person-re-identification.
- Redmon, J. and Farhadi, A. (2018). Yolov3: An incremental improvement. *arXiv preprint arXiv:1804.02767*.
- Ristani, E., Solera, F., Zou, R., Cucchiara, R., and Tomasi, C. (2016). Performance measures and a data set for multi-target, multi-camera tracking. In *European conference on computer vision*, pages 17–35. Springer.
- Sumari, F. O., Machaca, L., Huaman, J., Clua, E. W., and Guérin, J. (2020). Towards practical implementations of person re-identification from full video frames. *Pattern Recognition Letters*, 138:513–519.
- Szegedy, C., Vanhoucke, V., Ioffe, S., Shlens, J., and Wojna, Z. (2015). Rethinking the Inception Architecture for Computer Vision. *arXiv:1512.00567 [cs]*. arXiv: 1512.00567.
- Wang, G., Yuan, Y., Chen, X., Li, J., and Zhou, X. (2018). Learning Discriminative Features with Multiple Granularities for Person Re-Identification. *Proceedings of the 26th ACM international conference on Multimedia*, pages 274–282. arXiv: 1804.01438 version: 1.
- Wang, H., Gong, S., Zhu, X., and Xiang, T. (2016). Human-in-the-loop person re-identification. In *European conference on computer vision*, pages 405–422. Springer.
- Xiao, T., Li, S., Wang, B., Lin, L., and Wang, X. (2017). Joint detection and identification feature learning for person search. In *Proceedings of the IEEE Conference*

- on *Computer Vision and Pattern Recognition*, pages 3415–3424.
- Yang, C., Qi, F., and Jia, H. (2021). Survey on unsupervised techniques for person re-identification. In *2021 2nd International Conference on Computing and Data Science (CDS)*, pages 161–164. IEEE.
- Ye, M., Shen, J., Lin, G., Xiang, T., Shao, L., and Hoi, S. C. (2021). Deep learning for person re-identification: A survey and outlook. *IEEE Transactions on Pattern Analysis and Machine Intelligence*.
- Zhao, F., Liao, S., Xie, G.-S., Zhao, J., Zhang, K., and Shao, L. (2020). Unsupervised domain adaptation with noise resistible mutual-training for person re-identification. In *European Conference on Computer Vision*, pages 526–544. Springer.
- Zheng, L., Bie, Z., Sun, Y., Wang, J., Su, C., Wang, S., and Tian, Q. (2016). Mars: A video benchmark for large-scale person re-identification. In *European Conference on Computer Vision*, pages 868–884. Springer.
- Zheng, L., Shen, L., Tian, L., Wang, S., Wang, J., and Tian, Q. (2015a). Scalable person re-identification: A benchmark. In *Proceedings of the IEEE international conference on computer vision*, pages 1116–1124.
- Zheng, L., Shen, L., Tian, L., Wang, S., Wang, J., and Tian, Q. (2015b). Scalable person re-identification: A benchmark. In *Proceedings of the IEEE international conference on computer vision*, pages 1116–1124.
- Zheng, L., Zhang, H., Sun, S., Chandraker, M., Yang, Y., and Tian, Q. (2017). Person re-identification in the wild. In *Proceedings IEEE Conference on Computer Vision and Pattern Recognition*, pages 1367–1376.
- Zhong, Z., Zheng, L., Kang, G., Li, S., and Yang, Y. (2017). Random Erasing Data Augmentation. *arXiv:1708.04896 [cs]*. arXiv: 1708.04896.
- Zhuang, W., Wen, Y., Zhang, X., Gan, X., Yin, D., Zhou, D., Zhang, S., and Yi, S. (2020). Performance optimization of federated person re-identification via benchmark analysis. In *Proceedings of the 28th ACM International Conference on Multimedia*, pages 955–963.